CHEMISTRY
AN ASIAN JOURNAL

www.chemasianj.org

Accepted Article

Title: Mechanochemical Reactivity of a 1,2,4-triazoline-3,5-dione-Anthracene Diels-Alder Adduct

Authors: Hao-Chun Chang, Min-Chieh Liang, Chelsea Davis, Chia-chih Chang, and Van-Sieu Luc

To be cited as: *Chem. Asian J.* **2023**, e202300850

Link to VoR: https://doi.org/10.1002/asia.202300850

A Journal of

ACES Asian Chemical Editorial Society

WILEY VCH

10.1002/asia.202300850

WILEY VCH

COMMUNICATION

Mechanochemical Reactivity of a 1,2,4-triazoline-3,5-dione-Anthracene Diels-Alder Adduct

Hao-Chun Chang[a,b], Min-Chieh Liang[a,b], Van-Sieu Luc[a,c,d],, Chelsea Davis[e] and Chia-Chih Chang*[a,b]

[a] Department of Applied Chemistry, National Yang Ming Chiao Tung University, Hsinchu, Taiwan
No. 1001, Daxue Rd. East Dist., Hsinchu City 300093, Taiwan
[b] Center for Emergent Functional Matter Science, National Yang Ming Chiao Tung University, Hsinchu 300093, Taiwan
[c] Sustainable Chemical Science and Technology (SCST), Taiwan International Graduate Program (TIGP), Academia Sinica, Taipei 11529, Taiwan;
[d] Institute of Chemistry, Academia Sinica, Taipei 11529,, Taipei 11529, Taiwan
[e] Department of Mechanical Engineering, University of Delaware, Newark, Delaware 19716, U.S.A.
E-mail: cchang113ac@nycu.edu.tw
Supporting information for this article is given via a link at the end of the document

Abstract: Force-responsive molecules that produce fluorescent moieties under stress provide a means for stress-sensing and material damage assessment. In this work, we report a mechanophore based on Diels-Alder adduct **TAD-An** of 4,4'-(4,4'-diphenylmethylene)-bis-(1,2,4-triazoline-3,5-dione) and initiator-substituted anthracene that can undergo retro-Diels-Alder (rDA) reaction by pulsed ultrasonication and compressive activation in bulk materials. The influence of having C-N versus C-C bonds at the sites of bond scission is elucidated by comparing the relative mechanical strength of **TAD-An** to another Diels-Alder adduct **MAL-An** obtained from maleimide and anthracene. The susceptibility to undergo rDa reaction correlates well with bond energy, such that C-N bond containing **TAD-An** degrades faster C-C bond containing **MAL-An** because C-N bond is weaker than C-C bond. Specifically, the results from polymer degradation kinetics under pulsed ultrasonication shows that polymer containing **TAD-An** has a rate constant of 1.59×10^{-5} min^{-1}, while **MAL-An** (C-C bond) has a rate constant of 1.40×10^{-5} min^{-1}. Incorporation of **TAD-An** in a crosslinked polymer network demonstrates the feasibility to utilize **TAD-An** as an alternative force-responsive probe to visualize mechanical damage where fluorescence can be "turned-on" due to force-accelerated retro-Diels-Alder reaction.

Introduction

Mechanophores are force-sensitive motifs that can harness externally applied mechanical energy and trigger programmable chemical outputs.[1] Force-promoted twisting of the potential energy surfaces imparts distinctive mechanochemical activity to mechanophores, resulting in interesting mechanistic insights into various chemical reactions.[2] Unlike conventional polymers of which are known to undergo nonspecific bond scission under stress, mechanophore-embedded polymers can respond to mechanical forces selectively and trigger chemical changes at specific locations. The key concept of polymer mechanochemistry is to exploit the ability of polymer chains to transmit the stress and to enable facile activation of elegantly designed mechanophores. Notable examples include polymer backbone remodeling,[3] stress sensing,[4] stress strengthening,[5] flex-activated chemical reactions,[6] gated mechanochromism,[7] small molecule release,[8] drug delivery[9] and on-demand polymer degradation.[10] Assessment of material deformation and damage by the means of quantifying the change in fluorescence before and after provide a useful approach to realize the potential utilities of mechanophore in real materials. Mechanical stress can be then visualized through the emergence of colored and/or fluorescence species after mechanical impact.[11] For instance, force-induced 6-π electrocyclic ring-opening of spiropyran and napthothopyran to highly colored merocyanines in bulk materials have been demonstrated by several research groups.[12]

The availability of various mechanophores that can respond to either low-force (*e.g.,* ~200-300 pN for spiropyrans)[13] or high-force (*e.g.,* ~1-3 nN for mechanophores containing C-C bonds) regimes is of crucial importance for quantifying stress distribution and underpinning force transduction mechanism. Force-accelerated retro-Diels-Alder (rDA) reaction of anthracene adducts represents a promising platform for developing new mechanophores suitable for stress-sensing related applications because the optical properties (i.e., absorption range, fluorescence, quantum yield, and fluorescence lifetime) as well as force threshold required for mechanical activation can be further adjusted through molecular engineering of anthracene derivatives.[14] Noting that the bond energy of C-N bonds (*i.e.,* 305 kJ/mol) are smaller than that of C-C bonds (*i.e.,* 346 kJ/mol), we rationalize a Diels-Alder adduct featuring C-N bonds could result in a lower force threshold than the adduct featuring C-C at the sites of bond scission. To our delight, literature precedent by Lehn and coworkers has reported several successful examples of Diels-Alder reaction between N-phenyl-1,2,4-triazoline-3,5-dione (N-phenylTAD) and various anthracene derivatives and they demonstrated that the substituents on the C-9 and C-10 positions of anthracenes dictate the stability of corresponding Diels-Alder adducts.[15]

1,2,4-triazoline-3,5-dione (TAD) based derivatives are known to undergo many important classes of reactions including Diels-Alder reactions, Alder-ene reactions, electrophilic aromatic substitutions and [2+2]-cycloadditions.[16] Although Gossweiler *et al.* has reported the Diels-Alder adduct of N-phenylTAD and anthracene (An) can undergo flex-activated rDA to release small molecule N-phenylTAD in 2014,[6b] the mechanochemical reactivity of TAD-An with tethered polymer chains on TAD and An has not been reported elsewhere. Other TAD-derived mechanophores such as TAD-indole adducts have been integrated into polymer networks as force-reversible crosslink points to increase tensile strength, ductility and adaptability,

10.1002/asia.202300850

where C-N bond can be selectively cleaved as the mechanism for energy dissipation and TAD-indole adduct can radically re-form to restore mechanical integrity.[17] Given the high reactivity of TAD, one can envision that mechanophores that produce reactive TAD hold tremendous potentials for designing new materials featuring autonomous healing and strengthening properties.

Herein, we reported another Diels-Alder adduct of TAD and An, which is later referred as **TAD-An** and its chemical structure is shown in **Figure 1**, by reacting 4,4'-(4,4'-diphenylmethylene)-bis-(1,2,4-triazoline-3,5-dione) with an anthracene derivative (compound **1** as shown in **Scheme 1**) containing initiator suitable for subsequent attachment of polymers through controlled radical polymerization; the mechanochemical reactivity of **TAD-An** was compared to the previously reported Diels-Alder adduct of maleimide and anthracene (**MAL-An**) by measuring polymer degradation kinetics under pulsed ultrasonication. Furthermore, **TAD-An** was incorporated into a crosslinked poly(*N,N*-dimethylacrylamide) (PDMA) network to demonstrate the susceptibility to mechanical activation by rDA and the presence of as-formed anthracene motifs were readily observed under UV irradiation. Our research suggests promising opportunities for future exploration and utilization of **TAD-An** across diverse fields, with a particular focus on force-responsive materials and polymer chemistry. The unique reactivities of TAD derivatives and their adducts hold the promise of opening doors to innovative applications and materials designs.

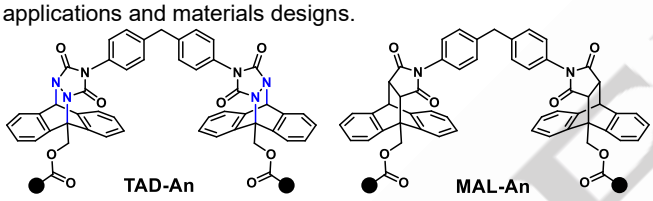

Figure 1. Diels-Alder adduct motifs of TAD-An and MAL-An studied as mechanophores.

Results and Discussion

We employed density functional theory (DFT) calculations to examine the mechanochemical behavior of the **TAD-An**. The constrained geometries simulate external force (CoGEF) technique was used at the B3LYP/6-31G* level of theory; starting from the equilibrium geometry of the unconstrained molecule, we artificially constrained the distance between the terminal methyl carbon atoms of **TAD-An**, and obtained the corresponding minimized energies at increasing distance increments of 0.05 Å. The computational results revealed that the mechanical elongation at the C-N bonds are preferred (as illustrated in **Figure 2a**), suggesting the feasibility of rDA reaction to produce the expected anthracene and TAD fragments. The maximum force at rupture (F_{max}) for the rDA reaction was calculated to be 3.55 nN, and the bond dissociation energy, representing the highest relative energy level just before bond breakage (E_{max}), was determined to be 195.17 kJ/mol. Notably, these values are less than that observed for the **MAL-An** (i.e., F_{max} = 4.24 nN, E_{max} = 313.14 kJ/mol) (as illustrated in **Figure 2b**, see **Figure S1** and **S2** in the SI for details).

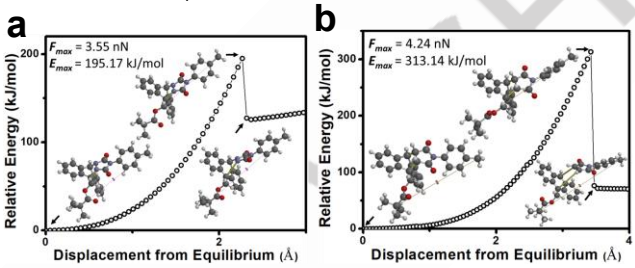

Figure 2. CoGEF result for (a) TAD-An and (b) MAL-An at the B3LYP/6-31G* level of DFT.

Diels-Alder reaction between compound **1** and 4,4'-(4,4'-diphenylmethylene)-bis-(1,2,4-triazoline-3,5-dione) (MDI-TAD) was carried out at room temperature to afford the target compound **2** in 90% yield. MDI-TAD was chosen because the ease of synthesis relative to the derivative containing only one TAD group. Incorporation of 2-bromo-2-methylpropionate in compound **1** enables subsequent attachment of polymer chains on both sides of **TAD-AN** via copper wire mediated controlled radical polymerization. In addition, we are intrigued by several reports on polymers containing two mechanophores at the middle of the chains and we intended to evaluate if two mechanochemical events on a single polymer chain can occur simultaneously. In order to incorporate **TAD-An** into crosslinked polymer network for the evaluation of mechanochemical reactivity in bulk materials, another diacrylate functionalized **TAD-An** derivative was synthesized by reacting diol-functionalized **TAD-An** with acrylic anhydride to afford the target compound **4** in 54% yield. Compound **5** was synthesized by reacting compound 1 with 4,4'-Methylenebis(N-phenylmaleimide) to provide insights on

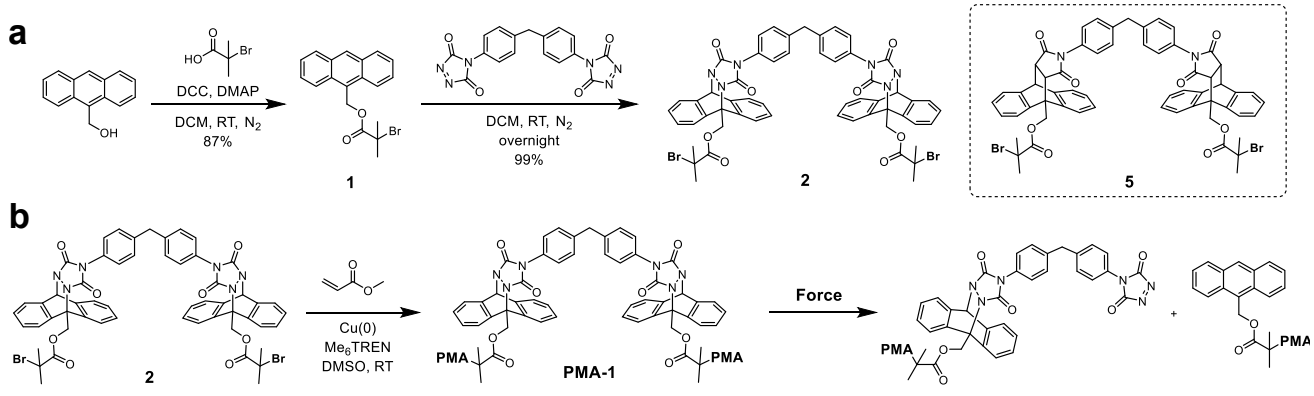

Scheme 1. (a) Synthesis of mechanophore containing initiators 2, 5, (b) Synthesis of PMA-1 and the expected rDA event induced by force.

10.1002/asia.202300850

relative mechanical strength of Diels-Alder adducts containing C-N and C-C bonds.

We attached poly(methyl acrylate) (PMA) chains to mechanophore containing initiators **2** and **5** by copper wire mediated controlled radical polymerization of methyl acrylate in DMSO, affording **PMA-1** (M_n = 103 kDa and Đ = 1.1) and **PMA-2** (M_n = 94 kDa and Đ = 1.1). The mechanochemical reactivities of the **TAD-An** and **MAL-An** were evaluated by subjecting **PMA-1** and **PMA-2** to pulsed ultrasound (1 s ON/ 1 s OFF, 8.23 W/cm^2) in tetrahydrofuran under a nitrogen atmosphere in an ice water bath. Aliquots were taken from the ultrasonication vessel and analyzed by gel permeation chromatography (GPC) equipped with a refractive index (RI) detector and the overlay of GPC traces is shown in **Figure 3a**. It is evident that the main peak weight at 19.5 min and the higher molecular weight shoulder peak at 18.0 min decreased noticeably. The shoulder peak at 18.0 min has a M_p of 204 kDa can be attributed to coupling reaction during polymerization because its molecular weight is twice as large as the M_p at 19.5 min (*i.e.,* 105 kDa). Most chains were cleaved at or near the center as evidenced by the emergence of a peak at 21.0 min with a M_p of 56 kDa. We also noted that another shoulder peak at 22.7 min began to appear as sonication time increased, which can be attributed a second scission event because the peak at 22.7 min corresponds to a M_p of 28 kDa. Furthermore, we observed a gradual increase in fluorescence intensity of aliquots obtained at different time points, coinciding with the reduction in molecular weight from approximately 100 kDa to 45 kDa (**Figure 3b**). The UV/vis spectrum of sonicated **PMA-1** was obtained from the GPC's photodiode array detector (**Figure 3c**) and compared with the UV/Vis spectrum of 9-anthracenemethyl acetate (**Figure S3**), the characteristic absorption of anthracene confirmed the formation of anthracene as expected from rDa of **TAD-An**. To provide a qualitative sense on the extent of rDa reaction, the stacked GPC RI and UV traces is shown **Figure 3d** and **Figure S4**; **PMA-1** lacks UV absorption (grey dash line) at 366nm, a wavelength selected for characteristic UV absorption for anthracene, before sonication and **PMA-1** becomes UV-absorbing at 366nm after sonication. The GPC trace obtained from UV detector at a wavelength of 366nm shows a monomodal distribution, while GPC trace obtained from RI detector shows a bimodal distribution with a higher molecular weight shoulder, indicating that a fraction of polymers either underwent non-specific chain scission or remained intact during pulsed ultrasonication. **PMA-1** obtained after 120 min sonication was analyzed by ^{1}H NMR spectroscopy, and the new peaks between 8.0 ppm and 8.6 ppm provides evidence for the presence of anthracene moieties (**Figure S6**). An excessive amount of freshly distilled cyclopentadiene CPD was also added to confirm the formation of TAD owing to fast reaction between CPD and TAD,[16, 18] the appearance of a new peak at 6.45 ppm in ^{1}H NMR spectrum matched with the chemical shifts of a TAD-CPD model compound synthesized independently, indicating the formation of TAD moiety as the result of force-accelerated rDA reaction (**Figure S7**). The thermal stability of **TAD-An** was estimated by heating compound **2** in DMSO-d6 at different temperatures and such adduct is stable up to 75°C, indicating lower reaction barrier for rDA reaction relative to conventional **MAL-An** adduct of which undergo rDA at 250°C; an activation barrier of 50.6 kcal/mol for rDA reaction of TAD-AN was estimated from the corresponding Arrhenius plot (**Figure S8**). Additionally, we established a calibration curve with 9-anthracenemethyl acetate (**Figure S9-S14**) and found that that the activation efficiency of **PMA-1** after 120 minutes was approximately 88% after conducting the experiments in triplicate on different days (**Table S1**). The calculation details are included in SI and polymer concentration was used as the denominator in the calculation. The activation efficiency is defined as the amount of anthracene-terminated daughter fragment relative to the initial amount of polymer chains present in the solution. Specifically, an activation efficiency of 200% would be obtained if all the TAD-AN units present in **PMA-1** underwent rDA reactions and produced TAD- and anthracene-terminated daughter fragments; the second TAD-AN becomes mechanochemically inactive when the first TAD-AN is cleaved because the remaining TAD-AN now becomes the chain-ends and the force experienced by polymer chain ends becomes the least during pulsed ultrasonication, which is less likely to be sufficient for inducing rDA reactions. Noting that Robb and coworkers have determined activation efficiency of **MAL-An** containing PMA with M_n in the range of 60.2-221 kDa to be approximately 96%,[19] our results implied that the likelihood only one side of **TAD-An** can be cleaved during each chain scission event, however, we could not completely rule out the possibility that two mechanochemical events on a single polymer chain can still occur simultaneously.

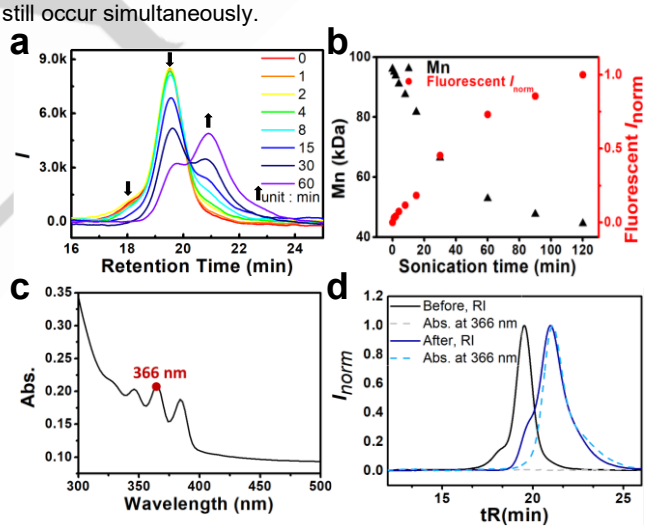

Figure 3. (a) GPC traces (RI) of PMA-1 solution (2.0 mg/mL in THF) upon pulsed ultrasonication at different times. (b) Upon ultrasonication, PMA-1 exhibited a reduction in molecular weight accompanied by an increase in fluorescent intensity. (c) UV/vis spectra of sonicated PMA-1 (extracted from the PDA detector of the GPC). (d) The stacked GPC traces present the normalized absorbance at 366 nm alongside the normalized RI-trace before sonication and after 120 minutes of sonication.

Next, we conducted kinetic analysis by assuming ultrasonication-induced chain scission process is a unimolecular reaction following a first-order mechanism.[20] Because second scission events after 60 minutes sonication time became more pronounced, we extracted polymer degradation rate constant based on the molecular weight data collected within the first 30 minutes of sonication. Recent work by Robb and coworkers have

10.1002/asia.202300850

demonstrates the initial rates method is an useful technique for rapid characterization of rate constants of which avoids complications associated with non-specific chain scission events.[21] The polymer degradation rate constant of **PMA-1** is 1.59×10^{-5} min^{-1} and the degradation rate constant of **PMA-2** is 1.40×10^{-5} min^{-1} (for further details, refer to **Figure S16-S25** and **Table S2-S11** in the SI). For mechanophore-free PMA synthesized from ethyl 2-bromo-2-methylpropionate, the degradation rate is determined to be 9.78×10^{-6} min^{-1}, which is much lower than **PMA-1** and **PMA-2**. Taken together, the degradation rate constant for **PMA-1** is 14% higher than that of **PMA-2** and 62% higher than **PMA**. Furthermore, the degradation rate constant for **PMA-2** is 43% higher than **PMA**. It is noteworthy the that degradation rate constant of **PMA-1** is determined to be 1.35×10^{-5} min^{-1} if the data from the first 60 minutes of sonication is used, which is 15% less than the rate constant of **PMA-1** in the first 30 minutes (see **Figure S26-S28** and **Table S12-S15** in the SI for details). This phenomenon could be attributed to the occurrence of second scission events observed from GPC RI traces, suggesting that we need to be cautious about the ultrasonication time period selected when analyzing polymer degradation kinetics during pulsed ultrasonication. Another method to determine rate constant is by tracking RI intensity change at a fixed elution time, which corresponds to the extent of chain scission of polymers at a fixed molecular weight during sonication. By applying the method reported by the Boydston group,[22] We determined the polymer degradation kinetics as follows: **PMA** exhibits a rate of 9.91×10^{-3} min^{-1}, **PMA-1** exhibits a rate of 1.53×10^{-2} min^{-1} and **PMA-2**, the degradation constant was 1.27×10^{-2} min^{-1} when the dataset from the initial 30 minutes was used (for detailed information, refer to **Figure S29-S41** and **Table S16** in the SI). Specifically, the polymer degradation kinetics of **PMA-1** are 20% higher than that of **PMA-2** and 54% higher than **PMA**; the polymer degradation kinetics of **PMA-2** are 28% higher than that of **PMA**. The polymer degradation rate constants of **PMA-1** were higher than those of **PMA-2** obtained by both analysis methods. This observation shows that the difference in bond energy was able to cause a variation in the rDA reaction rate, further influencing the disparity in polymer degradation kinetics.

In order to evaluate whether **TAD-An** is suitable to function as a mechanophore in bulk materials, incorporation of diacrylate functionalized crosslinker **4** into a polymer network was achieved through 2-hydroxy-4'-(2-hydroxyethoxy)-2-methylpriophenone (Irgacure 2959) initiated photopolymerization of dimethylacrylamide, resulting in the formation of **TAD-An** embedded network **PDMA-1**. (**Scheme S11**; Experimental details are provided in the SI). Upon compression of the nonfluorescent **PDMA-1** in a pellet press (369.4 MPa), fluorescence can be observed under 365nm UV light due to the formation of anthracene due to rDA reaction (**Figure 4**). As a control experiment to demonstrate that covalent integration of **TAD-AN** into PDMA network is important for compression activation, compound 2, a **TAD-AN** containing compound that cannot participate in photocrosslinking reaction, was used instead of crosslinker **4** to afford **PDMA-2** and we did not observe notable fluorescence after compression (**Figure S43**). Heating **PDMA-2** at 100°C and 110°C for 2 hours resulted in the appearance of notable fluorescence owing to thermally induced rDA reaction of **TAD-AN**.

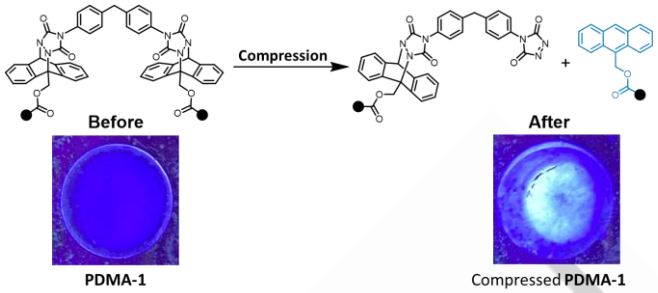

Figure 4. Compression of TAD-An containing polymer network can result in retro-Diels-Alder reaction of TAD-An; the photographs of as-prepared PDMA-1 (diameter: 14.83 mm, thickness: 4.14 mm) and compressed PDMA-1 under 365 nm UV light demonstrates the feasibility to visual mechanical damage.

In summary, we have successfully designed and synthesized a novel mechanophore based on Diels-Alder adduct **TAD-An**. Upon mechanochemical activation, this mechanophore can undergo rDA reaction, resulting in the formation of anthracene and triazolinedione fragments. By comparing the polymer degradation kinetics against the reference mechanophore **MAL-An** and mechanophore-free **PMA** under pulsed ultrasonication, the relative mechanical strength is established. We observed that the degradation rate of **TAD-An** was approximately 14%-20% faster than **MAL-An** and 54%-62% faster than mechanophore-free **PMA** depending on the analytical method used. The susceptibility to undergo rDa reaction correlates well with bond energy, such that C-N bond containing **TAD-An** degrades faster C-C bond containing **MAL-An** because C-N bond is weaker than C-C bond. We believe that this innovative mechanophore design paves the way for developing advanced mechanochemically responsive materials and provides valuable reference for the design of mechanophores.

Supporting Information

Synthetic details and the data that support the finds of this study are available in the supplementary material of this article.

Acknowledgements

This work is supported by the Young Scholar Fellowship Program of the National Science and Technology Council, Taiwan, under Grant 111-2636-E-A49 -015, and the Center for Emergent Functional Matter Science of National Yang Ming Chiao Tung University from the Featured Areas Research Center Program within the framework of the Higher Education Sprout Project by the Ministry of Education in Taiwan. We thank Dr. Li-Ching Shen (Center for Advanced Instrumentation at NYCU) for assistance with NMR experiments (MOST 111-2731-M-A49-001)

Keywords: retro-Diels-Alder reaction • polymer mechanochemistry • stress-sensing • 1,2,4-triazoline-3,5-dione

Reference

[1] a) Y. Chen, G. Mellot, D. van Luijk, C. Creton, R. P. Sijbesma, *Chem. Soc. Rev.* **2021**, *50*, 4100; b) N. Willis-Fox, E. Rognin, T. A. Aljohani, R. Daly, *Chem* **2018**, *4*, 2499; c) B. A. Versaw, T. Zeng, X. Hu, M. J. Robb, *J. Am. Chem. Soc.* **2021**, *143*, 21461.

[2] a) A. G. Roessler, P. M. Zimmerman, *J. Phys. Chem. C* **2018**, *122*, 6996; b) J. Ribas-Arino, M. Shiga, D. Marx, *Angew. Chem. Int. Ed.* **2009**, *48*, 4190.

[3] a) Z. S. Kean, S. L. Craig, *Polymer* **2012**, *53*, 1035; b) T. Matsuda, R. Kawakami, R. Namba, T. Nakajima, J. P. Gong, *Science* **2019**, *363*, 504; c) R. Groote, R. T. M. Jakobs, R. P. Sijbesma, *Polym. Chem.* **2013**, *4*, 4846; d) A. L. B. Ramirez, Z. S. Kean, J. A. Orlicki, M. Champhekar, S. M. Elsakr, W. E. Krause, S. L. Craig, *Nat. Chem.* **2013**, *5*, 757.

[4] a) A. R. Sulkanen, J. Sung, M. J. Robb, J. S. Moore, N. R. Sottos, G.-y. Liu, *J. Am. Chem. Soc.* **2019**, *141*, 4080; b) B. A. Beiermann, S. L. B. Kramer, J. S. Moore, S. R. White, N. R. Sottos, *ACS Macro Lett.* **2012**, *1*, 163; c) B. A. Beiermann, D. A. Davis, S. L. B. Kramer, J. S. Moore, N. R. Sottos, S. R. White, *J. Mater. Chem.* **2011**, *21*, 8443; d) M. Stratigaki, R. Göstl, *ChemPlusChem* **2020**, *85*, 1095.

[5] a) C. L. Brown, S. L. Craig, *Chem. Sci.* **2015**, *6*, 2158; b) J. Wang, I. Piskun, S. L. Craig, *ACS Macro Lett.* **2015**, *4*, 834; c) C. E. Diesendruck, J. S. Moore, in *Self‐Healing Polymers*, **2013**, pp. 193.

[6] a) M. B. Larsen, A. J. Boydston, *J. Am. Chem. Soc.* **2013**, *135*, 8189; b) G. R. Gossweiler, G. B. Hewage, G. Soriano, Q. Wang, G. W. Welshofer, X. Zhao, S. L. Craig, *ACS Macro Lett.* **2014**, *3*, 216; c) H. Shen, M. B. Larsen, A. G. Roessler, P. M. Zimmerman, A. J. Boydston, *Angew. Chem. Int. Ed.* **2021**, *60*, 13559; d) B. Cao, N. Boechler, A. J. Boydston, *Polymer* **2018**, *152*, 4; e) S. Nijem, Y. Song, R. Schwarz, C. E. Diesendruck, *Polym. Chem.* **2022**, *13*, 3986.

[7] a) A. C. Overholts, W. Granados Razo, M. J. Robb, *Nat. Chem.* **2023**, *15*, 332; b) R. W. Barber, M. J. Robb, *Chem. Sci.* **2021**, *12*, 11703; c) J. Kida, K. Imato, R. Goseki, D. Aoki, M. Morimoto, H. Otsuka, *Nat. Commun.* **2018**, *9*, 3504.

[8] a) Y. Lin, T. B. Kouznetsova, S. L. Craig, *J. Am. Chem. Soc.* **2020**, *142*, 99; b) Y. Lu, H. Sugita, K. Mikami, D. Aoki, H. Otsuka, *J. Am. Chem. Soc.* **2021**, *143*, 17744; c) R. Küng, R. Göstl, B. M. Schmidt, *Chemistry – A European Journal* **2022**, *28*, e202103860.

[9] a) X. Hu, T. Zeng, C. C. Husic, M. J. Robb, *ACS Cent. Sci.* **2021**, *7*, 1216; b) S. Huo, P. Zhao, Z. Shi, M. Zou, X. Yang, E. Warszawik, M. Loznik, R. Göstl, A. Herrmann, *Nat. Chem.* **2021**, *13*, 131; c) R. Küng, T. Pausch, D. Rasch, R. Göstl, B. M. Schmidt, *Angew. Chem. Int. Ed.* **2021**, *60*, 13626.

[10] a) T.-G. Hsu, S. Liu, X. Guan, S. Yoon, J. Zhou, W.-Y. Chen, S. Gaire, J. Seylar, H. Chen, Z. Wang, J. Rivera, L. Wu, C. J. Ziegler, R. McKenzie, J. Wang, *Nat. Commun.* **2023**, *14*, 225; b) Y. Lin, T. B. Kouznetsova, S. L. Craig, *J. Am. Chem. Soc.* **2020**, *142*, 2105; c) T.-G. Hsu, J. Zhou, H.-W. Su, B. R. Schrage, C. J. Ziegler, J. Wang, *J. Am. Chem. Soc.* **2020**, *142*, 2100.

[11] a) C. S. Davis, M. L. Rencheck, J. W. Woodcock, R. Beams, M. Wang, S. Stranick, A. M. Forster, J. W. Gilman, *ACS Appl. Mater. Interfaces* **2021**, *13*, 55498; b) J. A. Gohl, T. J. Wiley, H.-C. Chang, C.-C. Chang, C. S. Davis, *Frontiers in Soft Matter* **2023**, *3*.

[12] a) M. J. Robb, T. A. Kim, A. J. Halmes, S. R. White, N. R. Sottos, J. S. Moore, *J. Am. Chem. Soc.* **2016**, *138*, 12328; b) M. E. McFadden, M. J. Robb, *J. Am. Chem. Soc.* **2021**, *143*, 7925; c) D. A. Davis, A. Hamilton, J. Yang, L. D. Cremar, D. Van Gough, S. L. Potisek, M. T. Ong, P. V. Braun, T. J. Martínez, S. R. White, J. S. Moore, N. R. Sottos, *Nature* **2009**, *459*, 68; d) T. A. Kim, M. J. Robb, J. S. Moore, S. R. White, N. R. Sottos, *Macromolecules* **2018**, *51*, 9177.

[13] Y. Lin, M. H. Barbee, C.-C. Chang, S. L. Craig, *J. Am. Chem. Soc.* **2018**, *140*, 15969.

[14] a) C. P. Kabb, C. S. O'Bryan, C. D. Morley, T. E. Angelini, B. S. Sumerlin, *Chem. Sci.* **2019**, *10*, 7702; b) X. Wang, Y. Cao, Y. Peng, L. Wang, W. Hou, Y. Zhou, Y. Shi, H. Huang, Y. Chen, Y. Li, *ACS Macro Lett.* **2022**, *11*, 310; c) R. Göstl, R. P. Sijbesma, *Chem. Sci.* **2016**, *7*, 370.

[15] N. Roy, J.-M. Lehn, *Chemistry – An Asian Journal* **2011**, *6*, 2419.

[16] K. De Bruycker, S. Billiet, H. A. Houck, S. Chattopadhyay, J. M. Winne, F. E. Du Prez, *Chem. Rev.* **2016**, *116*, 3919.

[17] M. Du, H. A. Houck, Q. Yin, Y. Xu, Y. Huang, Y. Lan, L. Yang, F. E. Du Prez, G. Chang, *Nat. Commun.* **2022**, *13*, 3231.

[18] P. Mondal, P. K. Behera, N. K. Singha, *Prog. Polym. Sci.* **2021**, *113*, 101343.

[19] A. C. Overholts, M. J. Robb, *ACS Macro Lett.* **2022**, *11*, 733.

[20] H.-Y. Duan, Y.-X. Wang, L.-J. Wang, Y.-Q. Min, X.-H. Zhang, B.-Y. Du, *Macromolecules* **2017**, *50*, 1353.

[21] M. E. McFadden, A. C. Overholts, S. K. Osler, M. J. Robb, *ACS Macro Lett.* **2023**, *12*, 440.

[22] G. I. Peterson, A. J. Boydston, *Macromol. Rapid Commun.* **2014**, *35*, 1611.

10.1002/asia.202300850

WILEY VCH

COMMUNICATION

Graphical Abstract:

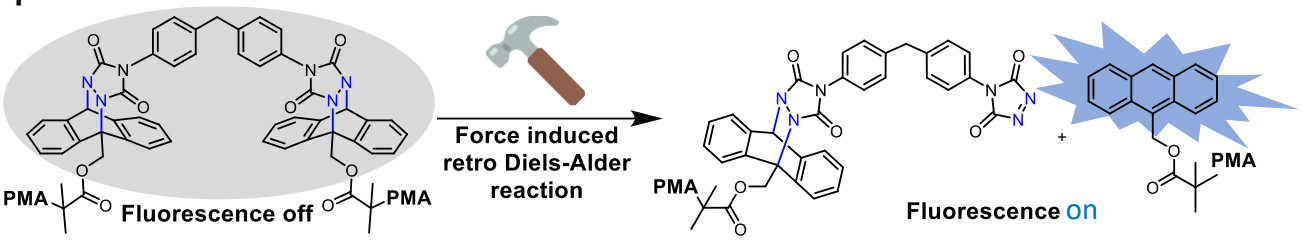

Text for TOC:

In this work, we report a mechanophore based on Diels-Alder adduct **TAD-An** of 4,4'-(4,4'-diphenylmethylene)-bis-(1,2,4-triazoline-3,5-dione) and initiator-substituted anthracene that can undergo retro-Diels-Alder reaction by pulsed ultrasonication and compressive activation in bulk materials. The susceptibility to undergo rDa reaction correlates well with bond energy, such that C-N bond containing **TAD-An** degrades faster C-C bond containing **MAL-An** because C-N bond is weaker than C-C bond. Incorporation of **TAD-An** in a crosslinked polymer network demonstrates the feasibility to utilize **TAD-An** as an alternative force-responsive probe. Compression of **TAD-An** embedded polymer network results in the emergence of fluorescence from newly formed anthracene functionality due to force-accelerated retro-Diesl Alder reaction.